Tethered Constrained-Geometry Catalysts in Mesoporous Silica: Probing the Influence of the "Second Sphere" on Polymer Properties

Sandra L. Burkett,* Stephen Soukasene, Kelly L. Milton, Ryan Welch, and Alicia J. Little

Department of Chemistry, Amherst College, P.O. Box 5000, Amherst, Massachusetts 01002

Rajeswari M. Kasi and E. Bryan Coughlin*

Department of Polymer Science and Engineering, University of Massachusetts, 120 Governors Drive, Amherst, Massachusetts 01003

Received January 20, 2005. Revised Manuscript Received March 21, 2005

The titanium catalyst $(C_5(CH_3)_4Si(CH_3)_2NR)TiCl_2$ has been tethered to the interior pore surfaces of *p*-aminophenylsilyl-functionalized mesoporous silica materials in a single-step process to form supported constrained-geometry catalysts (CGCs), and the polymerization of ethylene and copolymerization of ethylene and 1-octene by the resulting heterogenized CGCs have been studied. Confirmation that the intended supported CGC is correctly assembled and is the only catalytically active species is provided by spectroscopic characterization (^{29}Si CP MAS NMR) and by ethylene/1-octene copolymerization. The use of tailored mesoporous silica supports with different uniform pore sizes (25−70 Å) permits investigation of the influence of the structure of the support matrix (i.e., the "second sphere of influence", where the ligand environment provides the primary influence) on catalyst activity and on product properties. Homopolymerization of ethylene by the supported CGCs shows a clear trend in the crystallinity of the high-density polyethylene (HDPE) produced, with a higher degree of crystallinity observed for HDPE formed by the heterogenized CGC within the smaller-pore substrates. The observation that a "second sphere of influence" is indeed significant introduces an additional tunable parameter for the tailored synthesis of polyolefins using supported catalysts.

Introduction

Transition metal catalysis plays a central role in a multitude of chemical transformations such as the polymerization of olefins. The classification of these catalysts as either homogeneous or heterogeneous is generally made on the basis of solubility, or lack thereof, in the reaction solvent. Homogeneous catalysts are utilized extensively in the research laboratory due to their ease of use, overall activity, and high selectivity. However, the challenges of efficient product separation and catalyst recycling or recovery are often ignored when operating at the benchtop scale, although these considerations are of paramount significance for industrial-scale applications. The development of homogeneous single-site catalysts (SSCs) for the controlled polymerization of olefins has been the focus of considerable research for more than two decades.[1−3] For homogeneous single-site olefin polymerization catalysts, including the family of cyclopentadienyl- and amido-based constrained-geometry catalysts (CGCs),[4] the relationship of the transition metal with its associated ligand framework (i.e., the primary ligand architecture) to the resulting polymer properties (e.g., molecular weight, stereoregularity, and, in the case of copolymerization, comonomer distribution) is well-established.[5,6] Similarly, the influences exerted by the cocatalysts used in homogeneous olefin polymerizations are being elucidated through the design of tailored cocatalysts.[7] Concurrent work on olefin polymerization in the commercial sector has been targeted toward optimization of heterogeneous Ziegler−Natta catalysts for the production of commodity thermoplastics such as high-density polyethylene (HDPE), linear low-density polyethylene (LLDPE), and isotactic polypropylene. The current confluence of these two research developments is heterogenization of homogeneous SSCs, with the goal of combining the advantages of homogeneous and heterogeneous systems for the preparation of tailored polyolefins.[8]

A large number of articles and reviews regarding supported SSCs for olefin polymerization have been published in the past few years. Examples of matrixes on which SSCs, including CGCs, have been supported include silica,[9−16]

* To whom correspondence should be addressed. Sandra L. Burkett: Tel., (413) 542-2730; fax, (413) 542-2735; e-mail, slburkett@amherst.edu. E. Bryan Coughlin: Tel., (413) 577-1616; fax, (413) 545-0082; e-mail, coughlin@mail.pse.umass.edu.

(1) Brintzinger, H. H.; Fischer, D.; Mulhaupt, R.; Rieger, B.; Waymouth, R. M. *Angew. Chem., Int. Ed. Engl.* **1995**, *34*, 1143.
(2) Coates, G. W. *Chem. Rev.* **2000**, *100*, 1223.
(3) Resconi, L.; Cavallo, L.; Fait, A.; Piemontesi, F. *Chem. Rev.* **2000**, *100*, 1253.
(4) Chum, P. S.; Kruper, W. J.; Guest, M. J. *Adv. Mater.* **2000**, *12*, 1759.
(5) Alt, H. G.; Koppl, A. *Chem. Rev.* **2000**, *100*, 1205.
(6) Angermund, K.; Fink, G.; Jensen, V. R.; Kleinschmidt, R. *Chem. Rev.* **2000**, *100*, 1457.
(7) Chen, E. Y. X.; Marks, T. J. *Chem. Rev.* **2000**, *100*, 1391.
(8) Hlatky, G. G. *Chem. Rev.* **2000**, *100*, 1347.

10.1021/cm050137u CCC: $30.25
Published on Web 04/23/2005

mesoporous silica,[17−24] alumina,[9,10] and polystyrene.[25−27] These studies have focused primarily on methodologies for preparation of supported catalysts and on initial polymerization results (e.g., catalyst activity and polymer molecular weight and polydispersity). Polyolefins produced using SSCs that are confined within a porous support matrix show interesting physical properties compared to the polyolefins produced using the analogous unsupported catalysts; for example, they exhibit higher densities and greater percent crystallinity as a consequence of being formed as extended-chain fibers.[18,19] However, a comprehensive investigation of the fundamental influence of the support matrix (in other words, the "second sphere of influence") on catalytic performance and on the properties of the polyolefin product has not previously been reported; in particular, the effect of substrate pore size variation has not been explored, and previous studies have compared catalysts supported on nonporous substrates[9,11−16,25−27] or on a single substrate of uniform pore size[17−24] to the nonsupported analogues. Here, in order to explore the influences that an ordered, porous substrate has on the properties of the polyolefin product, primary-amine-functionalized mesoporous silica materials of varying pore diameter have been prepared and used as supports for tethered CGCs. Correlations of nascent polymer crystallinity and polymer molecular weight to the pore diameter of the support matrix have been established and are described herein.

Several features have gone into the design of the supported CGC system studied here, which is shown in Scheme 1. A key consideration in the selection of the catalyst tether is that the site for covalent attachment is remote from the catalytic site for olefin coordination and insertion. In addition, the tether must not be cleaved during the catalytic cycle. Consequently, CGCs are ideal candidates for heterogenization because it is possible to use the amido moiety as the linkage site. The catalyst can be assembled readily on the substrate via reaction of a substrate-bound primary amine

Scheme 1. Design Strategy for Preparation of the Functionalized Support and the Supported CGC

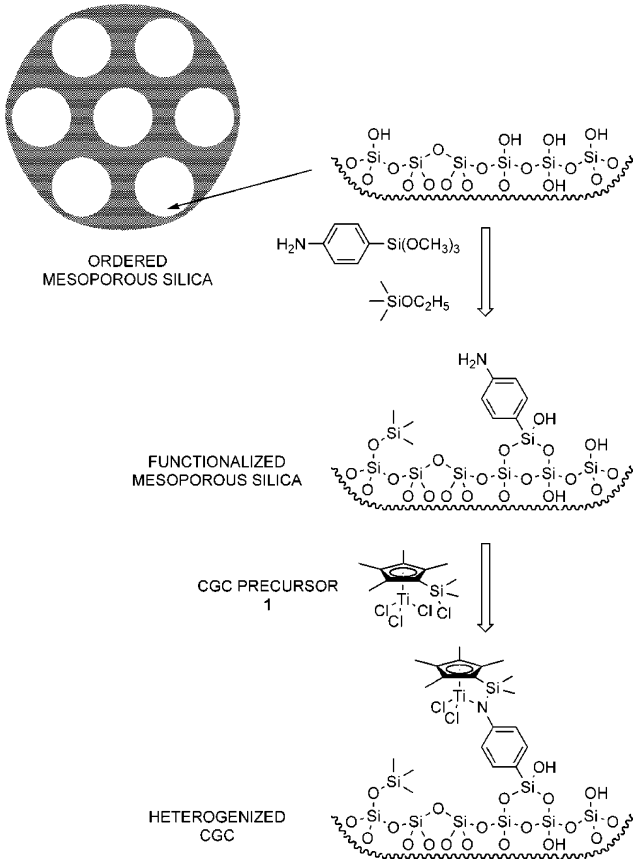

with the precursor titanium complex in a step that is directly analogous to a step in the synthesis of the nonsupported catalyst;[28,29] the success of this route for heterogenization of CGCs on (aminomethyl)polystyrene has been demonstrated previously.[26,27] This synthetic route avoids the incompletely assembled byproducts that have been problematic for other protocols used previously to tether CGCs to substrates.[10,12−14] An additional advantage of the CGC system studied here is that only catalyst molecules that are properly assembled on the substrate give rise to the desired polymerization chemistry; an incompletely assembled species exhibits different polymerization behavior that can be readily distinguished by product analysis.[26,27] Consequently, the polymerization studies provide a built-in assay for the identity of the surface-supported species.

The mesoporous silica substrates contain uniformly sized, well-ordered pores of sufficient size to accommodate the catalyst, reagent monomer, and product polymer. The sizes of the hexagonally arrayed cylindrical pores are tailored by the choice of surfactant used as the template in the synthesis (approximately 40 Å for hexadecyltrimethylammonium and approximately 70 Å for a poly(ethylene oxide)-*block*-poly(propylene oxide)-*block*-poly(ethylene oxide) triblock copolymer (Pluronic P123)). The uniformity of the pores within a given sample and the ability to tune pore size among samples permit examination of the extent to which pore size

(9) Collins, S.; Kelly, W. M.; Holden, D. A. *Macromolecules* **1992**, *25*, 1780.
(10) Galan-Fereres, M.; Koch, T.; Hey-Hawkins, E.; Eisen, M. S. *J. Organomet. Chem.* **1999**, *580*, 145.
(11) Lee, B. Y.; Oh, J. S. *Macromolecules* **2000**, *33*, 3194.
(12) Juvaste, H.; Pakkanen, T. T.; Iiskola, E. I. *Organometallics* **2000**, *19*, 1729.
(13) Juvaste, H.; Pakkanen, T. T.; Iiskola, E. I. *Organometallics* **2000**, *19*, 4834.
(14) Juvaste, H.; Pakkanen, T. T.; Iiskola, E. I. *J. Organomet. Chem.* **2000**, *606*, 169.
(15) Tian, J.; Soo-Ko, Y.; Metcalfe, R.; Feng, Y. D.; Collins, S. *Macromolecules* **2001**, *34*, 3120.
(16) Britcher, L.; Rahiala, H.; Hakala, K.; Mikkola, P.; Rosenholm, J. B. *Chem. Mater.* **2004**, *16*, 5713.
(17) Tudor, J.; O'Hare, D. *Chem. Commun.* **1997**, 603.
(18) Kageyama, K.; Tamazawa, J.; Aida, T. *Science* **1999**, *285*, 2113.
(19) Tajima, K.; Aida, T. *Chem. Commun.* **2000**, 2399.
(20) Tajima, K.; Ogawa, G.; Aida, T. *J. Polym. Sci., Part A: Polym. Chem.* **2000**, *38*, 4821.
(21) Ye, Z. B.; Alsyouri, H.; Zhu, S. P.; Lin, Y. S. *Polymer* **2003**, *44*, 969.
(22) Ye, Z. B.; Zhu, S. P.; Wang, W. J.; Alsyouri, H.; Lin, Y. S. *J. Polym. Sci., Part B: Polym. Phys.* **2003**, *41*, 2433.
(23) McKittrick, M. W.; Jones, C. W. *J. Am. Chem. Soc.* **2004**, *126*, 3052.
(24) Yu, K.; McKittrick, M. W.; Jones, C. W. *Organometallics* **2004**, *23*, 4089.
(25) Roscoe, S. B.; Fréchet, J. M. J.; Walzer, J. F.; Dias, A. J. *Science* **1998**, *280*, 270.
(26) Kasi, R. M.; Coughlin, E. B. *Organometallics* **2003**, *22*, 1534.
(27) Kasi, R. M.; Coughlin, E. B. *Organometallics* **2003**, *22*, 3792.
(28) Ciruelos, S.; Cuenca, T.; Gomez, R.; GomezSal, P.; Manzanero, A.; Royo, P. *Organometallics* **1996**, *15*, 5577.
(29) Royo, B.; Royo, P.; Cadenas, L. M. *J. Organomet. Chem.* **1998**, *551*, 293.

affects the properties of the polymers produced by the supported CGCs. Silanol groups on the pore surfaces permit functionalization with amine-containing organosiloxanes, which provide a route for introduction of catalyst linkage sites. Combinations of two organosiloxanes are used in this work: *p*-aminophenyltrimethoxysilane provides the site for covalent attachment of the catalyst, and either methyltriethoxysilane or trimethylethoxysilane is used to cap additional silanol groups and to increase the organophilicity of the pores.

Experimental Section

Methods. The two-, four-, or six-letter sample designations are explained in the Results and Discussion section.

Structural characterization of the mesostructured silica samples was performed by X-ray powder diffraction (XRD) using a Scintag XDS-2000 diffractometer with Cu Kα radiation.

Solid-state NMR spectra were obtained using a Bruker DSX300 spectrometer, with samples contained in 7 mm zirconia rotors. ^{13}C spectra were recorded at 75.48 MHz using cross polarization (CP) and magic angle spinning (MAS) at a rate of 4−5 kHz, and the chemical shift data is referenced to tetramethylsilane at 0 ppm. ^{29}Si spectra were recorded at 59.63 MHz, either without (silica substrates) or with (supported CGCs) CP, using MAS at a rate of 2.5−3.0 kHz, and the chemical shift data is referenced to sodium 3-(trimethylsilyl)propionate at 1.5 ppm. Deconvolution of the ^{29}Si MAS NMR spectra was performed using Bruker Xedplot software.

Infrared spectra were obtained using a Bruker IFS66 spectrometer, with samples prepared as potassium bromide pellets.

Nitrogen adsorption was performed using a Quantachrome Autosorb instrument. Surface area values were obtained by BET analysis. Pore size data, which is reported as the mode of the values for the pore diameter, was obtained by density functional theory analysis of the desorption curve.[30]

Elemental analysis of the functionalized silica samples was performed using Exeter Analytical 240XA CHN analyzers. A Leeman Labs Dual View DRE Sequential ICP was used to determine the Ti content of the supported CGC samples.

Polymer molecular weight (M_W) and polydispersity index (PDI) were determined by gel permeation chromatography (GPC) using a Polymer Laboratories PL-220 high-temperature GPC instrument equipped with a Wyatt MiniDawn (620 nm diode laser) high-temperature light scattering and refractive index detector. GPC was performed at 135 °C using 1,2,4-trichlorobenzene as the solvent. A (dn/dc) value of −0.11 was used for polyethylene. Calibration was performed using polystyrene standards.

Differential scanning calorimetry (DSC) was performed using a TA DSC 2910 instrument equipped with a liquid nitrogen cooling accessory unit under a continuous nitrogen purge (50 mL min^{-1}). The melting temperatures (T_M) for the ethylene/1-octene copolymers were obtained from the second melt using a heating and cooling scan at 10 °C min^{-1}, and the T_m values were used to determine the 1-octene content.[31] The melting temperatures for polyethylene were obtained from the first melt using a heating and cooling scan at 10 °C min^{-1}. The heats of fusion (ΔH_f) for the ethylene/1-octene copolymers and polyethylene were obtained from the first melt using a heating and cooling scan at 10 °C min^{-1}. The percent crystallinity of the polyethylene was determined from the ratio of the heat of fusion of the polymer to the heat of fusion of a single crystal of polyethylene (293 J g^{-1}).

Incorporation of 1-octene in the ethylene/1-octene copolymers was confirmed by ^{13}C NMR spectroscopy of the polymers in solution at 120 °C using 1,1,2,2-tetrachloroethane-d_2 as the lock solvent. The integrated intensities of the hexyl branch resonances relative to the polyethylene backbone resonances were used to quantify the 1-octene content of the copolymer.[32]

Synthesis of Smaller-Pore Mesoporous Silica Materials (HX, HC). In a typical synthesis,[33] 2.88 g of hexadecyltrimethylammonium bromide (Aldrich) was dissolved in a solution prepared from 130 g of water (EasyPure UF, 18 MΩ) and 1.35 g of 50 wt % aqueous sodium hydroxide (Alfa) in a PTFE jar. With vigorous stirring, 10.00 g of tetramethoxysilane (Aldrich) was added quickly. The reaction vessel was sealed and the sample was stirred at room temperature for 24 h and then heated statically at 90 °C for 24 h. The product was collected by vacuum filtration, washed with water, and dried in air at room temperature.

Surfactant removal was performed either by extraction or by calcination. In the extraction procedure, a suspension of 4 g of sample in 500 mL of methanol that contained 7 g of concentrated hydrochloric acid was heated to reflux for 24 h, and the product was collected by vacuum filtration, washed with methanol, and dried in air at room temperature. In the calcination procedure, the sample was heated in a muffle furnace under static conditions to 650 °C at a rate of 1 °C min^{-1} and then heated at 650 °C for 6 h.

Synthesis of Larger-Pore Mesoporous Silica Materials (PX, PC). In a typical synthesis,[34] 4.00 g of Pluronic P123 ($(CH_2CH_2O)_{20}$-$(CH_2(CH_3)CH_2O)_{70}(CH_2CH_2O)_{20}$); BASF) was dissolved in a solution prepared from 105 g of water and 24 g of concentrated hydrochloric acid in a PTFE jar. With vigorous stirring, 8.54 g of tetraethoxysilane (Aldrich) was added quickly. The reaction vessel was sealed and the sample was shaken at 35 °C for 24 h and then heated statically at 100 °C for 28 h. The product was collected by vacuum filtration, washed with water, and dried in air at room temperature.

Surfactant removal was performed either by extraction or by calcination. In the extraction procedure, 5 g of sample was extracted for 24 h with 500 mL of refluxing ethanol in a Soxhlet apparatus, and the product was collected by vacuum filtration, washed with ethanol, and dried in air at room temperature. In the calcination procedure, the sample was heated to 650 °C at a rate of 1 °C min^{-1} and then heated at 650 °C for 6 h.

Functionalization of Mesoporous Silica Samples. In a typical functionalization reaction,[35−37] 1 g of a smaller-pore mesoporous silica (HX or HC) was dried in vacuo at 80 °C, then transferred to a nitrogen atmosphere, and suspended in 100 mL of anhydrous toluene. After addition of 0.4 mL of water, the suspension was stirred for 1 h at room temperature. Meanwhile, 0.66 g of *p*-aminophenyltrimethoxysilane (Gelest) was dissolved in 20 mL of anhydrous toluene under nitrogen and then added to the silica suspension when the hydration step was complete. Either 1.86 mL of methyltriethoxysilane (Aldrich) (for sample HX) or 1.52 mL of trimethylethoxysilane (Aldrich) (for sample HC) was added and the suspension was heated to reflux for 20 h. Approximately

(30) Thommes, M.; Köhn, R.; Fröba, M. *Appl. Surf. Sci.* **2002**, *196*, 239.
(31) Chen, H. Y.; Chum, S. P.; Hiltner, A.; Baer, E. *J. Polym. Sci., Part B: Polym. Phys.* **2001**, *39*, 1578.
(32) Randall, J. C. *J. Macromol. Sci.-Rev. Macromol. Chem. Phys.* **1989**, *C29*, 201.
(33) Lim, M. H.; Stein, A. *Chem. Mater.* **1999**, *11*, 3285.
(34) Zhao, D.; Feng, J.; Huo, Q.; Melosh, N.; Fredrickson, G. H.; Chmelka, B. F.; Stucky, G. D. *Science* **1998**, *279*, 548.
(35) Feng, X.; Fryxell, G. E.; Wang, L.-Q.; Kim, A. Y.; Liu, J.; Kemmerr, K. M. *Science* **1997**, *276*, 923.
(36) Liu, J.; Feng, X. D.; Fryxell, G. E.; Wang, L. Q.; Kim, A. Y.; Gong, M. L. *Adv. Mater.* **1998**, *10*, 161.
(37) Fryxell, G. E.; Liu, J.; Hauser, T. A.; Nie, Z.; Ferris, K. F.; Mattigod, S.; Gong, M.; Hallen, R. T. *Chem. Mater.* **1999**, *11*, 2148.

60 mL of liquid was removed by azeotropic distillation, and the functionalized sample was collected by vacuum filtration, washed with toluene and ethanol, and dried in vacuo at 80 °C. For functionalization of larger-pore mesoporous silica (PX or PC), the amounts of water, *p*-aminophenyltrimethoxysilane, and methyltriethoxysilane or trimethylethoxysilane were reduced to approximately 75% of the above amounts due to the lower surface areas of these materials.

Qualitative Colorimetric Assay for Primary Amine. A yellow solution of bindone (ICI America) in glacial acetic acid was prepared at a concentration of 1 mg mL^{-1}. For the colorimetric assay, 10 mg of nonfunctionalized or functionalized mesoporous silica was combined with 1.0 mL of bindone solution. After 60 min, the solution was removed via pipet, and the solid was washed with 1.0 mL of water and then dried in air. The presence of a blue or violet color was indicative of the reaction of bindone with a primary aromatic amine.[38]

Assembly of CGC on Functionalized Mesoporous Silica Substrates (HXAM-Ti, HCAT-Ti, PXAM-Ti, PCAT-Ti). Synthesis of supported catalysts was performed under nitrogen in Schlenk glassware or in an inert atmosphere drybox. The titanium catalyst precursor (((chlorodimethylsilyl)tetramethylcyclopentadienyl)-titanium trichloride, **1**) was synthesized as reported previously.[26,27] The mole ratio of the amine content of the support to **1** was selected to be 3:1. Dry, distilled tetramethylethylenediamine (TMEDA; Aldrich) was used as a base to scavenge the hydrochloric acid formed as a byproduct.

In a typical reaction, 79.0 mg (0.22 mmol) of **1** was added to a slurry of sample PXAM (303.0 mg; 1.3 wt % N, 0.928 mmol N per 1 g of silica) in toluene. Following the addition of 0.1 mL (0.5 mmol) of TMEDA, the suspension was stirred at 60 °C for 3 d. The support was washed several times with toluene to remove soluble byproducts and residual **1**, and the supported catalyst was recovered and dried in vacuo at 60 °C for 12 h, which yielded 381.9 mg of supported catalyst PXAM-Ti.

Ethylene/1-Octene Copolymerization. In a typical reaction, 13.9 mg of PXAM-Ti was added to a solution containing 10.0 mL of toluene and 1.0 mL of 30 wt % methylalumoxane (MAO) in toluene (Albemarle) in a thick-walled polymerization reactor;[39] an excess of MAO cocatalyst was used to activate the CGC and to scavenge any ammonium salts that remained from the CGC assembly step. 1-Octene (5 mL, 50 vol % in toluene) was added by means of an additional cylinder, and ethylene was supplied at a pressure of 4 atm for 20 min at room temperature with constant stirring. The ethylene supply was stopped, the reactor was vented to remove excess ethylene, and the reaction mixture was quenched with a solution of 10 vol % hydrochloric acid in methanol. The polyethylene was filtered and dried in vacuo at 60 °C overnight to yield the ethylene/1-octene copolymer.

Ethylene Polymerization. In a typical reaction, 13.5 mg of PXAM-Ti was added to a solution containing 10.0 mL of toluene and 1.0 mL of 30 wt % MAO in toluene in a thick-walled polymerization reactor.[39] The reactor was pressurized with ethylene at 4 atm for 10 min at room temperature with constant stirring. The ethylene supply was stopped, the reactor was vented to remove excess ethylene, and the reaction mixture was quenched with a 10 vol % solution of hydrochloric acid in methanol. The polyethylene was filtered and dried in vacuo at 60 °C overnight.

(38) Vecera, M.; Gasparic, J. *Detection and Identification of Organic Compounds*; Plenum: New York, 1971.
(39) Constable, G. S.; Gonzalez-Ruiz, R. A.; Kasi, R. M.; Coughlin, E. B. *Macromolecules* **2002**, *35*, 9613.

Table 1. Structural Characterization of Mesoporous Silica Substrates

sample	d_{100} (Å)	d_{110} (Å)	d_{200} (Å)	a (Å)	surface area ($m^2\,g^{-1}$)	pore diameter (Å)	wall thickness (Å)
HX	42.6	24.4	21.1	48.9	893	43	6
HXAM	42.1	24.0	20.8	48.2	645	35	13
HC	36.5	20.8	18.0	41.8	826	32	10
HCAT	36.6	20.9	18.0	41.9	535	26	16
PX	99	57.3	49.6	114	571	70	44
PXAM	97	57.1	49.3	113	404	<70[a]	>43[a]
PC	97	55.9	48.2	112	617	>70[a]	<42[a]
PCAT	98	56.1	48.5	112	469	<70[a]	>42[a]

[a] See text.

Results and Discussion

Substrate Preparation and Characterization. The nonfunctionalized and functionalized mesoporous silica materials are designated by two- or four-letter names, respectively, that are indicative of the template (H: hexadecyltrimethylammonium bromide; P: Pluronic P123), the method of surfactant removal (X: solvent extraction; C: calcination), the amine source (A: *p*-aminophenyltrimethoxysilane), and the silanol capping group (M: methyltriethoxysilane; T: trimethylethoxysilane). Two different capping strategies were used, dependent on the hydroxyl content of the nonfunctionalized substrate. For extracted samples, trimethylethoxysilane was used as the silanol-capping reagent in order to achieve approximate monolayer coverage of functional groups on the silanol-rich pore surfaces; however, it should be noted that incomplete condensation of the alkoxy groups can also introduce silanol groups. For calcined samples, trimethylethoxysilane was used as the capping reagent due to the low initial density of surface silanol groups, which makes monolayer coverage difficult. The conventional capping reagent hexamethyldisilazane (HMDS) could not be used in conjunction with the *p*-aminophenyl functionality because silylation of the amine group occurs.

The hexagonal symmetry of each of the nonfunctionalized and functionalized silica materials is apparent from the three peaks in the X-ray powder diffraction pattern, which can be assigned as the (100), (110), and (200) reflections (Table 1). The lattice parameter a, which corresponds to the distance between the centers of adjacent pores, is calculated from d_{100} ($a = (2/\sqrt{3})d_{100}$). The pore-to-pore distances observed for the nonfunctionalized materials are consistent with published values, based on the template and the method of template removal.[33,34] Functionalization of the silica materials does not change the observed pore-to-pore spacing.

Nitrogen adsorption/desorption studies confirm that the nonfunctionalized and functionalized materials are mesoporous. The BET surface area values reported in Table 1 indicate that a decrease in surface area occurs upon introduction of functional groups, which suggests that the organic moieties are attached to the walls of the pores. For the samples prepared using the hexadecyltrimethylammonium template (HX, HC, HXAM, HCAT), a narrow distribution of pore diameters is observed, and the mode pore diameter value for each functionalized material is observed to be smaller than that of the nonfunctionalized parent material. For the samples prepared using the Pluronic P123 template

Table 2. ^{29}Si MAS NMR Analysis of Mesoporous Silica Substrate Composition

	relative integrated area of resonance[a,b]									
sample	Q^4 (-109 ± 1 ppm)	Q^3 (-100 ± 1 ppm)	Q^2 (-90 ± 2 ppm)	T^3_A (-78 ± 3 ppm)	T^2_A (-68 ± 1 ppm)	T^1_A (-61 ± 2 ppm)	T^3_M (-56 ± 3 ppm)	T^2_M (-51 ± 2 ppm)	T^1_M (-42 ± 3 ppm)	M^1_T (14 ± 1 ppm)
HX	49.4	47.6	3.0	0	0	0	0	0	0	0
HXAM	63.9	31.5	4.6	2.1	3.5	3.3	2.4	1.7	1.8	0
HC	61.6	36.6	1.8	0	0	0	0	0	0	0
HCAT	80.5	17.8	1.6	1.2	2.8	5.3	0	0	0	3.7
PX	51.8	40.5	7.7	0	0	0	0	0	0	0
PXAM	60.0	34.5	5.5	5.3	4.2	2.3	1.9	0.8	0.8	0
PC	68.4	29.3	2.3	0	0	0	0	0	0	0
PCAT	78.3	20.8	0.9	0.5	2.5	2.2	0	0	0	3.7

[a] $Q^n = Si(OSi)_n(OH)_{4-n}$; $T^n_A = Si(p\text{-}C_6H_4NH_2)(OSi)_n(OH)_{3-n}$; $T^n_M = Si(CH_3)(OSi)_n(OH)_{3-n}$; $M^n_T = Si(CH_3)_3(OSi)_n$. [b] Relative areas are reported such that a constant value of 100 is maintained for the inorganic silica content ($\sum_n$ area $(Q^n) = 100$).

Table 3. Analysis of Mesoporous Silica Substrate Composition

sample	Si−OH/Si ratio[a,b]	Si-cap/Si ratio[a,c]	Si-amine/Si ratio[a,d]	cap nm^{-2} [a,c]	amine nm^{-2} [a,d]	mmol amine g^{-1} [e]	bindone assay
HX	0.536	0	0	0	0	0	white
HXAM	0.489	0.051	0.078	0.67	1.02	0.57	blue
HC	0.402	0	0	0	0	0	white
HCAT	0.306	0.033	0.082	0.52	1.30	0.77	blue
PX	0.558	0	0	0	0	0	white
PXAM	0.493	0.031	0.103	0.62	2.09	0.93	blue
PC	0.340	0	0	0	0	0	white
PCAT	0.272	0.034	0.048	0.65	0.91	0.44	blue

[a] Determined by ^{29}Si MAS NMR. [b] Total silanol content, from Q^n ($n \leq 3$), T^n_A ($n \leq 2$), and T^n_T ($n \leq 2$). [c] Cap refers to T^n_T ($n \leq 3$) and T^n_M ($n \leq 1$). [d] Amine refers to T^n_A ($n \leq 3$). [e] Determined by elemental analysis.

(PX, PC, PXAM, PCAT), broader pore size distributions are observed. When the functional groups are introduced, a decreased population of larger pores (65−80 Å) and an increased population of smaller pores (50−60 Å) are observed, consistent with the location of these groups on the pore surfaces. An estimate of the wall thickness of each sample is obtained by comparison of the pore diameter and pore-to-pore distance. The wall thicknesses of the hexadecyltrimethylammonium-templated silica samples increase by approximately 6 Å upon functionalization, which is consistent with the formation of an incomplete monolayer on the pore surface. The broader distribution of pore diameters of the Pluronic P123-templated silica samples renders the analogous determination difficult.

Infrared spectroscopy confirms that *p*-aminophenyl moieties (1603 cm^{-1}, 1510 cm^{-1} (aromatic ring stretching))[40] are present in all of the functionalized samples. The methylsilyl groups (1275 cm^{-1} (CH_3 symmetric deformation)) of the HXAM and PXAM materials and the trimethylsilyl groups (2984 cm^{-1} (CH_3 asymmetric stretch), 850 cm^{-1} (Si−C rocking)) of HCAT and PCAT samples are also apparent.[40] The peaks attributed to the organic groups are weak relative to those attributed to Si−O−Si stretching (1000−1200 cm^{-1}) and to SiO−H stretching (3000−3700 cm^{-1}).

In the ^{13}C CP MAS NMR spectra of the functionalized samples, the *p*-aminophenyl moieties are indicated by a packet of four broad resonances: 114 ppm (*C* meta to C−Si), 120−130 ppm shoulder (*C*−Si), 135 ppm (*C* ortho to C−Si), and 148 ppm (*C*−NH_2). The significant breadth of the peaks and the presence of spinning sidebands are indicative of the rigidity of the organic moieties. The methylsilyl groups of the HXAM and PXAM samples are indicated by a resonance at −8 ppm, and the trimethylsilyl groups of the HCAT and PCAT samples are confirmed by a resonance at −2 ppm. A small amount of residual Pluronic P123 template (15 ppm; multiple resonances, 60−75 ppm) is detected in the PX and PXAM samples at long data acquisition times and is likely responsible for the small populations of small pores observed for these samples.

The degree of condensation of the silicate framework and the organosiloxane contents are determined by ^{29}Si MAS NMR. The resonances for the inorganic silicate units ($Q^n = Si(OSi)_n(OH)_{4-n}$) are well resolved from those for the *p*-aminophenylsiloxane species ($T^n_A = Si(C_6H_4NH_2)(OSi)_n(OH)_{3-n}$) and those for the methylsiloxane ($T^n_M = Si(CH_3)(OSi)_n(OH)_{3-n}$) or trimethylsiloxane ($M^n_T = Si(CH_3)_3(OSi)_n$) units.[41] The peak positions and relative integrated areas for each sample are reported in Table 2. The ^{29}Si NMR data permit determination of the total silanol content (Si−OH/Si ratio), the *p*-aminophenylsiloxane content (Si-amine/Si ratio), and the methylsiloxane or trimethylsiloxane capping group content (Si-cap/Si ratio) (Table 3). The silanol content of the nonfunctionalized materials depends on the method used for surfactant removal, with higher silanol contents observed for the nonfunctionalized, extracted materials compared to the nonfunctionalized, calcined materials. The total silanol content (Si−OH/Si ratio) decreases upon functionalization, even though the *p*-aminophenylsiloxane and methylsiloxane groups themselves introduce silanol groups (T^2 and T^1). The decrease in inorganic silanol content (Q^3 and Q^2) suggests that the surface silanol groups have been capped by the organosiloxane moieties. The protocol that uses the trimethylsiloxane capping group leads to a more substantial

(40) Socrates, G. *Infrared Characteristic Group Frequencies*; Wiley: New York, 1980.
(41) Liepins, E.; Zicmane, I.; Lukevics, E. *J. Organomet. Chem.* **1986**, *306*, 167.

Table 4. Preparation of Supported CGCs

sample	substrate (mg)	**1** (mg) [mmol]	supported catalyst (mg)	Ti (mmol g^{-1})
HXAM-Ti	514.9	75.0 [0.20]	571.0	0.35
HCAT-Ti	465.2	88.7 [0.24]	559.2	0.43
PXAM-Ti	303.0	79.0 [0.22]	381.9	0.56
PCAT-Ti	506.0	82.3 [0.22]	584.0	0.37

decrease in inorganic silanol content and to a smaller remaining organic silanol content in the sample than that in which methylsiloxane is introduced, with the consequence that these samples, prepared using calcined parent materials, have the lowest total silanol contents. The majority of these remaining silanol groups are inaccessible framework silanol groups rather than accessible surface silanol groups, as evidenced by the only modest additional decrease in Q^3 and Q^2 and lack of change in T^2 and T^1 that occur upon subsequent treatment of the functionalized samples with the conventional capping reagent HMDS (data not shown); HMDS-treated samples were not used as substrates for catalyst attachment, however, because silylation of the *p*-aminophenyl group also occurs.

Quantification of *p*-aminophenyl group content (amine nm^{-2}) and capping group content (cap nm^{-2}) is achieved by combining the ^{29}Si NMR data and the surface area values from BET (Table 3). The observation that there are approximately 2 organosiloxane moieties per nm^2 (or approximately half-monolayer coverage)[35] is consistent with the extent of coverage that can be estimated from the change in wall thickness.

Reaction with bindone provides a qualitative colorimetric assay for the accessibility and reactivity of the *p*-aminophenyl groups.[38] Upon treatment with the yellow bindone solution, all of the functionalized samples turn a deep blue color, which is indicative of the reaction of bindone with a primary aromatic amine to form an imine complex, and the supernatant remains yellow. By contrast, the nonfunctionalized samples remain white and the supernatant remains yellow. The results of the bindone assay confirm the availability of the tethered *p*-aminophenyl moieties for subsequent reactions.

Catalyst Preparation and Characterization. The CGC complex was assembled in a single step by reaction of the precursor titanium piano stool complex (**1**)[26,27] with the *p*-aminophenyl-functionalized silica substrates (HXAM, HCAT, PXAM, and PCAT); the experimental parameters are listed in Table 4. Formation of the intended CGC product PXAM-Ti was confirmed by the appearance of a new resonance between −23 ppm and −27 ppm in the ^{29}Si CP MAS NMR spectrum, which is consistent with the value reported for the dimethylsilyl moiety of the analogous homogeneous CGC;[42] this resonance is distinct from that observed for the precursor complex in solution (−5 ppm)[26,27] and from those observed for the tethered piano stool complexes that correspond to incompletely assembled CGCs (−5 ppm to −12 ppm).[12−14] Thus, the ^{29}Si NMR data suggest that the CGC is assembled correctly on the *p*-aminophenyl-functionalized silica substrate.

Table 5. Ethylene/1-Octene Copolymerization

sample	Ti (μmol)	activity (kg atm^{-1} $h^{-1}[Ti]^{-1}$)	$M_w(\times 10^{-5})$ (g mol^{-1})	PDI	T_m (°C)	1-octene incorporation (mol %)
HXAM-Ti	4.3	10.1	3.0	2.0	123.0	1.5
HCAT-Ti	7.1	9.8	2.1	2.9	122.0	1.5
PXAM-Ti	7.6	12.3	3.2	3.0	124.0	1.5
PCAT-Ti	4.0	12.5	2.9	3.8	123.0	1.5

Ethylene/1-Octene Copolymerization. The formation of copolymers of ethylene and 1-octene can be used as evidence to verify the complete and correct assembly of the CGC on the silica substrate. Homogeneous CGCs incorporate 1-octene during ethylene/1-octene copolymerization,[4] whereas the precursor complex (**1**) and the tethered, incompletely assembled CGCs polymerize ethylene but do not incorporate 1-octene.[26,27]

Copolymerization of ethylene and 1-octene was performed using the supported CGCs, with MAO as the cocatalyst. Catalyst activity and polymer characterization data for each system are reported in Table 5. The supported CGCs show lower activity compared to the homogeneous CGCs for ethylene/1-octene copolymerization. No dependence of catalyst activity on pore size or silanol content was observed. By contrast, the molecular weight of the product copolymers is dependent on the substrate pore size, with larger-pore materials affording copolymers of higher molecular weight, likely due to an influence of pore size on monomer diffusion to the catalytic sites.[43] The copolymers produced using the supported CGCs show broader PDI valves (2−4) than those produced using the analogous homogeneous CGCs, which is consistent with restricted diffusion of the monomers to the catalyst active sites.[43]

Polyethylene and polyethylene-based copolymers are semicrystalline materials that have well-documented melting endotherms. HDPE, which has fewer than 4 methyl branches per 1000 carbon atoms, has a melting temperature (T_m) of greater than 130 °C. By contrast, LLDPE, which is a copolymer of ethylene and 1-octene, has a depressed T_m value relative to HDPE due to disruption of the crystalline polyethylene domains by the comonomer branches. DSC of the product polymers reveals a melting endotherm for each sample at 122−124 °C, which can be attributed to the presence of 1-octene units within the polymer (Table 5). A linear correlation exists between the extent of 1-octene incorporation and the observed depression in melting point relative to the melting point of HDPE.[31] For the polymers synthesized using the supported CGCs, the 1-octene content was determined to be 1.5 mol %.

Incorporation of 1-octene also reduces the degree of crystallinity of the polymer relative to that of HDPE because the crystalline polyethylene domains are disrupted by the hexyl branches. The degree of crystallinity of LLDPE is quantified by the ratio of its heat of fusion (ΔH_f) to that of a single crystal of polyethylene (293 J g^{-1}). The low crystallinity values (approximately 8−10%) measured for the product polymers are suggestive of incorporation of 1-octene.

(42) Alt, H. G.; Reb, A.; Milius, W.; Weis, A. *J. Organomet. Chem.* **2001**, *628*, 169.

(43) Dotson, N. A.; Galvan, R.; Laurence, R. L.; Tirrell, M. *Polymerization Process Modeling*; John Wiley & Sons: New York, 1995.

Table 6. Ethylene Polymerization

sample	Ti (μmol)	activity (kg atm^{-1} h^{-1} [Ti]$^{-1}$)	M_w($\times 10^{-5}$) (g mol^{-1})	PDI	T_m (°C)	crystallinity (%)
HXAM-Ti	3.6	5.5	2.3	1.9	137.9	36.0
HCAT-Ti	7.2	43.7	2.0	2.7	134.8	27.0
PXAM-Ti	7.5	19.7	3.6	2.5	133.1	22.0
PCAT-Ti	3.5	28.8	3.9	2.0	133.7	23.7

The extent of 1-octene incorporation was also evaluated by solution ^{13}C NMR of the product polymers. The observation of resonances that correspond to hexyl branches confirms the incorporation of 1-octene.[32,44] The 1-octene content, which is calculated from the relative integrated intensity of the 1-octene resonances, was determined to be 1.5 mol %, which is consistent with the value obtained from the analysis of melting data.

In sum, only completely assembled CGCs within mesoporous silica give rise to the desired polymerization chemistry, namely, the formation of LLDPE. This polymerization behavior is in contrast to the polymerization behavior of incompletely assembled CGC species, which yield HDPE, which can be distinguished by product analysis.

Ethylene Homopolymerization. The effects of the primary ligand architecture of SSCs on the production of polyethylene of different molecular weights, branch contents, melting points, and degrees of crystallinity are well-studied. Polymerization of ethylene was investigated using the silica-supported CGCs in conjunction with MAO as the cocatalyst in order to evaluate the influence of the substrate (i.e., the "second sphere of influence") on the properties of the polymer produced. Previous ethylene homopolymerization studies using CGCs, metallocenes, and piano stool complexes tethered to inorganic and organic supports have indicated that, in general, catalyst activity is lower than that observed for the analogous homogeneous systems.[14,16,26,27] The molecular weight of the polyethylene produced is typically reduced, although in some cases the molecular weight can be dramatically higher.[18] Catalyst activity, polymer molecular weight, polydispersity index, polymer melting point, and percent crystallinity are reported in Table 6 for each system investigated here. With use of the silica-supported CGCs, it was observed that the activity for production of polyethylene is lower than that observed for analogous homogeneous catalysts. Polyethylene samples produced from the supported CGCs have polydispersity indices of 1.9−2.5, which are comparable to those of polyethylene produced from the analogous homogeneous CGCs. The molecular weight of the polyethylene is dependent on the substrate pore size, with larger-pore materials affording polymer of higher molecular weight. The lower molecular weights of the polymers formed by the smaller-pore systems can be attributed to limitations on diffusion of ethylene to the active sites.[43]

The polyethylene products have melting temperatures in the range of 133−137 °C and crystallinity values of 22−36%, which suggests that the crystallinity of these samples is lower than that of HDPE produced using homogeneous CGCs.[45] A similarly lowered degree of crystallinity has been observed for polyethylene synthesized using the CGC supported on (aminomethyl)polystyrene.[26,27] In the current system, however, the crystallinity of the polyethylene produced using the CGC supported on porous silica can be tuned by varying the pore size of the substrate, with a smaller-pore substrate giving rise to a higher degree of crystallinity than a larger-pore substrate. During the course of polymerization, growth of the polymer occurs from a metal-alkyl bond within the pore. As a consequence of polymer chain growth, the ethylene monomer is transformed into solid polyethylene. The resulting HDPE is comprised of crystalline domains, an intermediate domain (the interface between the crystalline and amorphous domains), and amorphous domains. When polyethylene is prepared from CGCs supported within smaller-pore substrates, there are fewer conformations that a polymer chain can adopt within the pore during formation. Hence, as the polymer chains are formed and forced out of the pores in a so-called "extrusion polymerization" process,[18] there is a higher degree of prealignment of polymer chains and thus a greater likelihood that these chains adopt the periodic arrangement characteristic of crystalline polyethylene. By contrast, for polyethylene produced from CGCs supported within larger-pore substrates, a greater number of conformations for the growing polymer chains is accessible. The larger number of chain conformations that are possible as the polymers exit from the pores results in fewer chains being properly aligned to generate a crystalline solid, which leads to an overall lower degree of crystallinity. The trend of smaller-pore matrixes leading to polyethylene with higher crystallinty and larger-pore matrixes yielding polyethylene with lower crystallinity demonstrates that there is indeed a "second sphere of influence" for these silica-supported CGCs.

Conclusion

Functionalized, ordered mesoporous silica materials provide well-defined support matrixes that have variable pore diameters for the assembly of supported CGCs. Formation of a correctly assembled, supported CGC is demonstrated clearly both by spectroscopic characterization and by product formation in ethylene/1-octene copolymerization to generate LLDPE. Homopolymerization of ethylene by CGCs supported in pores of variable diameter shows a clear trend in the crystallinity of the HDPE produced. The higher degree of crystallinity for samples produced from small-pore supports is a consequence of the limited number of possible conformations that the polymer chains can adopt within the pores, which leads to a greater likelihood of the formation of crystalline domains as the chains exit from the pores. Conversely, polyethylene formed from CGCs supported in larger-pore substrates has a lower degree of crystallinity due to the larger number of possible conformations that the chains can adopt prior to entering the solid state, and consequently the polymer is more likely to have a larger amorphous content. The ability of the support matrix to alter the physical properties of the polymer produced shows that a "second sphere of influence" is indeed significant. This observation

(44) Kimura, K.; Yuasa, S.; Maru, Y. *Polymer* **1984**, *25*, 441.

(45) Musikabhumma, K.; Spaniol, T. P.; Okuda, J. *Macromol. Chem. Phys.* **2002**, *203*, 115.

brings the exciting possibility that, in the future design of supported catalysts for tailored polymerization of olefins, there is an expanded number of tunable parameters.

Acknowledgment. The authors thank John Krohn (UMass) for performing the nitrogen adsorption experiments, Dr. Matthias Thommes (Quantachrome) for assistance with the analysis of the adsorption data, Dr. L. Charles Dickinson (UMass) for NMR assistance, and BASF for a sample of Pluronic P123. This material is based on work supported by the National Science Foundation under Grant No. CHE-0113643, by the Materials Research Society Undergraduate Materials Research Initiative, and by Amherst College through an award from the Undergraduate Biological Sciences Education Program of the Howard Hughes Medical Institute. Central analytical facilities used in these studies were supported by the NSF-sponsored Materials Research Science and Engineering Center on Polymers at UMass Amherst (DMR-0213695).

Supporting Information Available: ^{29}Si NMR spectra (PDF). This material is available free of charge via the Internet at http://pubs.acs.org.

CM050137U